"Physics of Auroral Phenomena", Proc. XXII Annual Seminar, Apatity, pp.45-48, 1999

Polar
Geophysical
Institute

FRACTAL APPROACH TO DYNAMICS OF AURORAL TV IMAGES

B.V. Kozelov (*Polar Geophysical Institute, Apatity, Russia*)

Introduction

During the last two decades the fractal geometry has become a powerful approach to the different physical problems. It is also found to be useful in image processing applications. A numerical quantity that characterises the auroral structure would be important for auroral investigations. We try to obtain the quantity on the base of box-counting dimension. In our preliminary treatments we discussed a possible calculation procedure to obtain a numerical quantity of auroral structure and applied it to several auroral images (*Kozelov and Kornilov*, 1997). We have also provided some tests of this procedure by simulated images (*Kozelov*, 1998) and long set of auroral all-sky TV frames (*Kozelov and Jussila*, 1999). In this paper we present application of our procedure to several long sets of digitised TV images obtained by camera with narrow field of view at Loparskaya station. Discussion of some results is also presented.

Data

For analysis we use TV recording obtained at Loparskaya observatory during winter 1993-1994 by camera with narrow field of view. The resolution of fine structure of auroral luminosity for this camera is higher than the one for usual all-sky camera. Unfortunately, the most part of the recording contains two kinds of misrepresentation: regular noise from other devices, and overscale for high intensities. We select 5 time intervals then these misrepresentations were absent and TV images contain different auroral structures. The TV frames during each interval have been digitised with resolution 255x255 pixels and 64 grey levels. In our calculations we used the central part of image without time and observatory labels.

Calculation procedure

The digitised frames presented as $(n \times m)$ - arrays have been processed by calculation procedure which based on box-counting method (*Feder*, 1988) and contains the following steps:

1). The rectangle region contained the auroral structure has been located.

2). The isoline of equal intensity $L(I)$ has been obtained for each grey level (intensity) I.

3). Using pixels as a mesh, the number $N(\delta,I)$ of boxes of side δ (δ = 1,2,4,…, min(n,m)), that overlap the isoline $L(I)$ has been counted.

4). The dimension $D(I)$ of isoline $L(I)$ is the logarithmic rate at which $N(\delta,I)$ increases as δ decreasing, and it has been estimated by the gradient of the graph of log $N(\delta,I)$ against the -log δ for each I.

By this procedure the dependence $D(I)$ has been calculated for each image. Unfortunately, we cannot normalise grey levels in digitised images on intensity in Rayleighs. Therefore we use only relative units of intensity I. As a result, the dependence $D(I,t)$ has been obtained for each sets of frames. Here I is an intensity level, and t is a time (or frame number in the set).

The box-counting dimension obtaining in calculation procedure is an estimation of fractal dimension (*Falconer*, page 38). However, the range of δ scales available in TV image is not large, therefore we say only about pre-fractal structure, not the fractal one, which supposes limit for $\delta \to 0$. In any case, the number of mesh boxes of side δ that intersect an isoline is an indication of how spread out or irregular the line is when examined at scale δ. The dimension reflects how rapidly the irregularities develop as δ decreasing. Theoretically the dimension of subset of plane may have a value in range from 0 (dimension of disconnected set of points) to 2 (dimension of plane figures). Dimension of a smooth line is equal to 1.

Results of calculations

Fig.1 presents the results for first interval and contains: a) dependence $D(I,t)$, where dimension presented by grey scale as a function of time and intensity; b) the maximal dimension of isoline on frame as a function of time; c) the most structured intensity (MSI, this is an intensity, for which isoline has the maximal dimension) as a function of time; d) several images from discussed set, time moments marked by T_0,T_1,T_2 at Fig.1c.

Fig.2 shows dependencies $D(I,t)$ for other analysed data intervals.

Comments and discussion

Case 1. (Fig.1) The image contains a stable arc with rays. In the beginning of the interval the arc is bright, ray structure is clear seeing, the maximal dimension D is equal to 1.45-1.5 for intensities 40-45. Gradually the arc intensity is decreasing, rays are smoothing, that leads to decreasing of the maximal dimension to D=1.35-1.4 and MSI to ≈30.

Case 2. (Fig.2a) Diffuse patches. During 130 seconds these patches have very changeable shape and location, but the MSI varies very smoothly in a small range. However, the maximal dimension varies in wide range from 1.73 to 1.88. We can conclude that the main changes occurred in structure of luminosity region, but not in its intensity. Several more intensive patches which occurred during 15-30 seconds and 50-80 seconds, are reflected at *D(I, t)* for $I > 35$ and were accompanied by decreasing of maximal dimension for $I < 35$. We can note that values of maximal dimension are higher than in first case.

Case 3. (Fig.2b) Diffuse luminosity. In the beginning of this interval the luminosity is like two very diffuse arcs, fine structure is not seen. During the first 250 seconds this luminosity has large variations of intensity and at 200 s it merges with background noise. The maximal dimension fluctuates smoothly in region 1.6-1.7 with period near 70 s. After 260 s large intensification of the luminosity has occurred, and small intensive patches has appeared, which leads to increasing of the maximal dimension to 1.85. Later the luminosity becomes the same form as in the beginning of the interval, and intensity is decreasing. One can see that in this case the variations of *D* and MSI values are essential but not directly correlated.

Case 4. (Fig.2c) During the first 5 seconds bright arc with diffuse region behind it, is moving from the middle of the image to the left. After this, two waves of intensification are moving along the arc, and intensity of the arc is gradually decreasing. On the *D(I, t)* plate one can see two region which have different dynamics. In the region of small intensities ($I < 20$) the smooth variations of maximal dimension (*D*=1.45-1.55) and MSI value. This region mainly characterises the diffuse region behind the arc. Next region on the *D(I, t)* plate with another dynamics one can see for $I > 20$. In this region the local maximum of dimension may be located (*D*=1.25-1.4). This maximum reflects the motion of bright forms at the image. So as the waves of intensification on the arc are retiring from the point of observation, we see its motion as a decreasing of the MSI value.

Case 5. (Fig.2d) Evolution of the arc on the diffuse background. As for case 4, one can select two regions on the *D(I, t)* plate. For $I < 25$ the maximal dimension is gradually increasing from *D*=1.7 to 1.8, the MSI value is also smoothly increasing. This region characterises the diffuse background. For $I > 25$ the *D(I, t)* plate reflects variation in arc structure. Initially (*t*=20:23:33) the arc is bright without fine structure, *D*=1.55. After 20:23:40 the most intensive region at the arc breaks into two parts, which become clearer (*D*=1.38). After 20:23:50 the arc is gradually breaking into a number of small rays, the dimension is increasing. Further, the number and intensity of the rays are decreasing. In the end of the interval the arc merges with background.

In Table we present the dimension ranges obtained for different auroral forms in discussed cases. The same device recorded all TV data used; therefore we have possibility to compare these values. Mainly one can see the assumed tendency: the dimension of the diffuse forms is higher than it is for discrete forms. One exception is only diffuse region behind the arc in case 4. More detailed study shows that isolines for $I<22$ in this case contain very large part from diffuse luminosity and large smooth part around the arc. The dimension is weighed average value; therefore it is lower in this case than in other cases. Corrected values (without part around the arc) presented in brackets.

Table. Dimension of the most structured isoline for different auroral forms obtained by Fig.1-5.

	Case 1	Case 2	Case 3	Case 4	Case 5
Diffuse luminosity	-	-	1.6-1.85	1.45-1.55 (1.55-1.72)	1.7-1.8
Diffuse patches	-	1.73-1.88	-	-	-
Arc with rays	1.4-1.5	-	-	-	1.55-1.65
Line arc	-	-	-	1.25-1.4	1.35-1.5

Conclusions

1) The dependence of *D(I)* as a function of image number (time) is sufficiently smooth one and allows us to use *D(I, t)* figure to follow dynamics of auroral images.

2) Maximums of *D(I)* are associated with auroral forms on the image. Variations of the maximum value and intensity, which corresponds to the maximum, reflect dynamics of auroral images from frame to frame.

3) The maximal dimensions of isoline for different auroral forms have assumed tendency: the dimension of the diffuse forms is higher than it is for discrete forms.

Acknowledgements. The author thanks V.Tagirov for data of TV observations and I.Kornilov for useful discussions.

References

Falconer K.J., Fractal geometry: mathematical foundations and applications. John Wiley & Sons, New York, 1995.

Feder J., Fractals, Plenum Press, New York, 1988.

Kozelov B.V., I.A.Kornilov, Fractal characteristics of digitised auroral TV images, in: "Physics of Auroral Phenomena", 20 Annual Seminar, 25 -28 February 1997. Abstracts, PGI-97-01-101, p.40, 1997.

Kozelov B.V., Search of scale parameters of auroral forms by TV measurements, in: "Physics of Auroral Phenomena", 21 Annual Seminar, 24-27 March 1998 Abstracts, PGI-98-01-104, p.57, 1998.

Kozelov B.V., Jussila J., Dynamics of pre-fractal structure of auroral all-sky TV images, Geophys. Res. Let. 1999 (submitted).

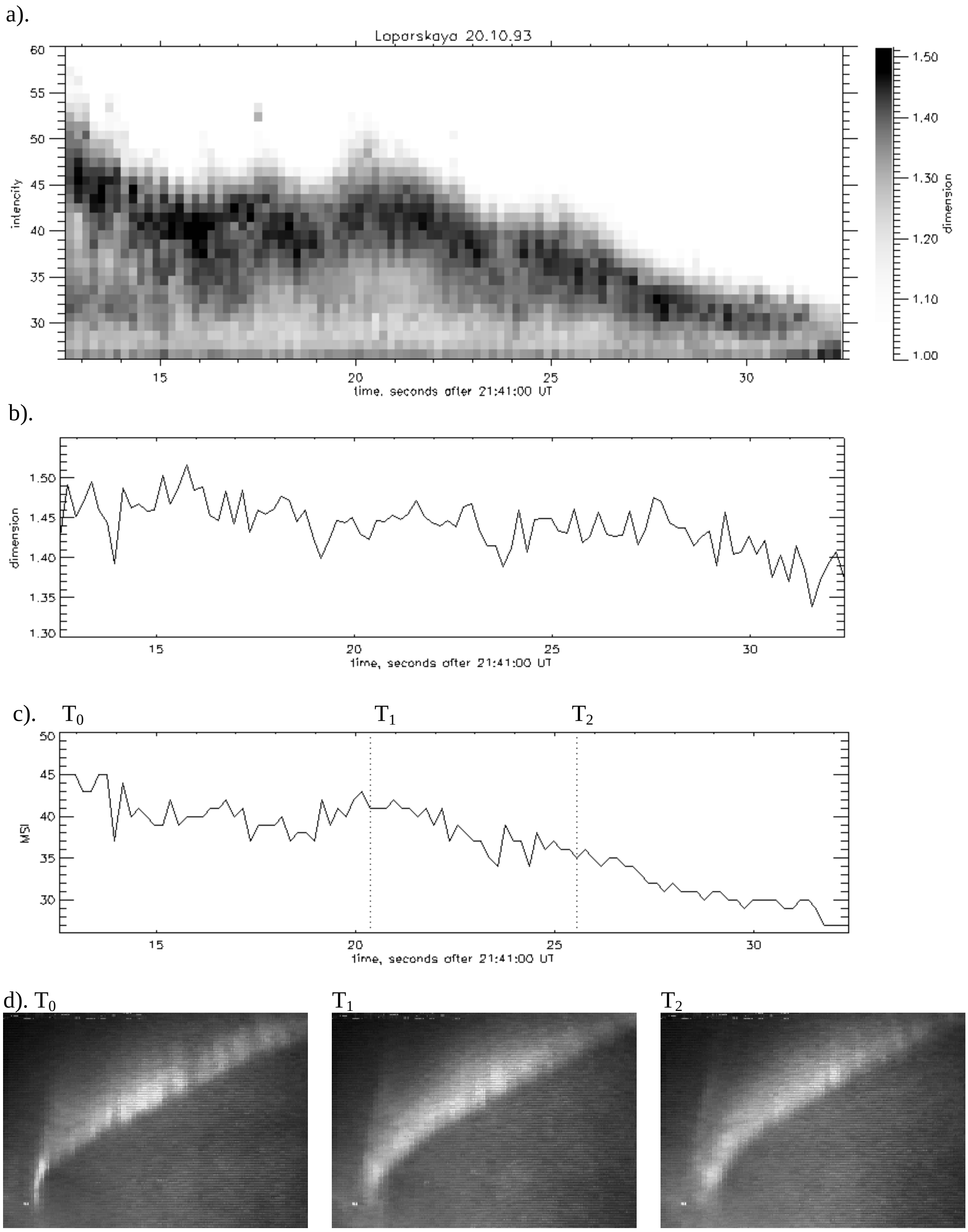
a).
Loparskaya 20.10.93
intencity
dimension
time, seconds after 21:41:00 UT
b).
dimension
time, seconds after 21:41:00 UT
c). T_0
T_1
T_2
MSI
time, seconds after 21:41:00 UT
d). T_0
T_1
T_2

Fig.1

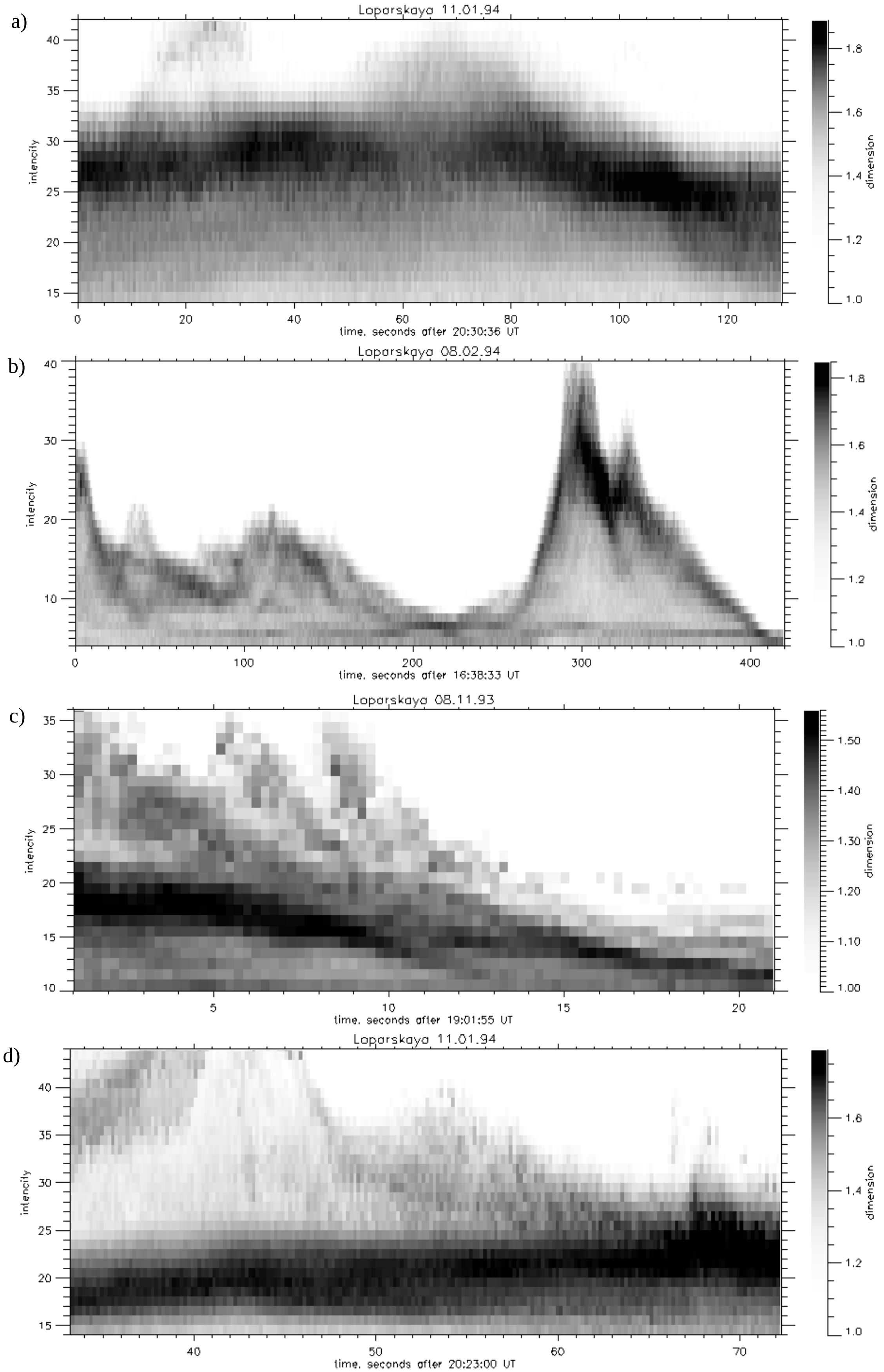
a)
Loparskaya 11.01.94
intencity
time, seconds after 20:30:36 UT
dimension
b)
Loparskaya 08.02.94
intencity
time, seconds after 16:38:33 UT
dimension
c)
Loparskaya 08.11.93
intencity
time, seconds after 19:01:55 UT
dimension
d)
Loparskaya 11.01.94
intencity
time, seconds after 20:23:00 UT
dimension

Fig.2